ARTICLE

Neurogenesis-dependent remodeling of hippocampal circuits reduces PTSD-like behaviors in adult mice

Risako Fujikawa[1,2], Adam I. Ramsaran[1,3], Axel Guskjolen[1,4], Juan de la Parra[1], Yi Zou[1], Andrew J. Mocle[1,4], Sheena A. Josselyn[1,3,4,5] and Paul W. Frankland[1,3,4,5,6]✉

Post-traumatic stress disorder (PTSD) is a hypermnesic condition that develops in a subset of individuals following exposure to severe trauma. PTSD symptoms are debilitating, and include increased anxiety, abnormal threat generalization, and impaired extinction. In developing treatment strategies for PTSD, preclinical studies in rodents have largely focused on interventions that target post-encoding memory processes such as reconsolidation and extinction. Instead, here we focus on forgetting, another post-encoding process that regulates memory expression. Using a double trauma murine model for PTSD, we asked whether promoting neurogenesis-mediated forgetting can weaken trauma memories and associated PTSD-relevant behavioral phenotypes. In the double trauma paradigm, consecutive aversive experiences lead to a constellation of behavioral phenotypes associated with PTSD including increases in anxiety-like behavior, abnormal threat generalization, and deficient extinction. We found that post-training interventions that elevate hippocampal neurogenesis weakened the original trauma memory and decreased these PTSD-relevant phenotypes. These effects were observed using multiple methods to manipulate hippocampal neurogenesis, including interventions restricted to neural progenitor cells that selectively promoted integration of adult-generated granule cells into hippocampal circuits. The same interventions also weakened cocaine place preference memories, suggesting that promoting hippocampal neurogenesis may represent a broadly useful approach in hypermnesic conditions such as PTSD and substance abuse disorders.

Molecular Psychiatry (2024) 29:3316–3329; https://doi.org/10.1038/s41380-024-02585-7

INTRODUCTION

Neurogenesis persists throughout adulthood in the subgranular zone of the dentate gyrus in mammals [1], including humans [2]. Over the course of several weeks, newly-generated granule cells become synaptically integrated into hippocampal circuits, receiving input connections from the entorhinal cortex and making output connections with CA3 pyramidal cells [3–5]. On the one hand, the addition of new neurons to hippocampal circuits facilitates the formation of new memories, likely via promoting pattern separation [6–9]. On the other, continuous remodeling of hippocampal circuits via integration of new neurons may additionally overwrite existing memories, rendering them harder to access [10–13]. Indeed, artificially elevating levels of hippocampal neurogenesis following learning produces forgetting of established hippocampus-dependent memories [14]. This form of neurogenesis-mediated forgetting is observed in a broad range of aversively- and appetitively-motivated rodent memory paradigms [14–22] that are generally considered to model adaptive memory. Here we ask whether promoting neurogenesis-mediated forgetting might similarly induce forgetting of maladaptive memories that underlie hypermnesic conditions, such as post-traumatic stress disorder (PTSD). PTSD is a psychiatric disorder that may occur in individuals who have experienced or witnessed a traumatic event or series of traumatic events. Symptoms include heightened anxiety, over generalization of threat responses to otherwise safe environments or situations, and reduced extinction of conditioned threat [23–25].

To model PTSD in mice, we used a double trauma PTSD paradigm developed by Finsterwald et al. [26]. This paradigm involves two traumatic events, with animals first trained in an inhibitory avoidance (IA) paradigm using a high intensity footshock (event 1). Subsequent presentation of a reminder shock in a different context (event 2) then leads to the emergence of a constellation of behaviors that mimic those observed in PTSD including increases in anxiety, threat generalization, and impaired extinction. In adult mice, we found that manipulating hippocampal neurogenesis post-training weakened the original IA memory and attenuated the anxiety, generalization and extinction phenotypes. These data suggest that targeting active forgetting mechanisms, such as hippocampal neurogenesis, is a promising strategy for developing new treatments for hypermnesic conditions such as PTSD.

MATERIALS/SUBJECTS AND METHODS

Animals

Mice. All procedures were approved by the Animal Care and Use Committee at the Hospital for Sick Children and conducted in

[1]Program in Neurosciences & Mental Health, Hospital for Sick Children, 555 University Avenue, Toronto, ON M5G 1X8, Canada. [2]Department of Molecular and System Pharmacology, Graduate School of Pharmaceutical Sciences, Kyushu University, Fukuoka 812-8582, Japan. [3]Department of Psychology, University of Toronto, Toronto, ON M5S 3G3, Canada. [4]Department of Physiology, University of Toronto, Toronto, ON M5G 1X8, Canada. [5]Institute of Medical Sciences, University of Toronto, Toronto, ON M5S 1A8, Canada. [6]Child & Brain Development Program, Canadian Institute for Advanced Research, Toronto, ON M5G 1M1, Canada. ✉email: paul.frankland@sickkids.ca

Received: 6 November 2023 Revised: 18 April 2024 Accepted: 23 April 2024
Published online: 8 May 2024

accordance with the policies of the Canadian Council on Animal Care (CCAC) and National Institutes of Health (NIH) Guidelines on the Care and Use of Laboratory Animals. All mice were bred and maintained at the Hospital for Sick Children on a 12 h light/dark cycle. Mice were weaned on postnatal day 21 and group-housed with same-sex littermates in standard mouse housing cages containing 2–5 mice each. Mice had *ad libitum* access to food and water throughout the duration of the experiments.

Multiple mouse lines were used for behavioral experiments. Unless otherwise stated, we used wild-type (WT) hybrid mice from a C57BL/6N x 129SvEv (Taconic Farms, Germantown, NY) cross. All mice were 8–12 weeks old at the start of the experiments.

Similar behavioral experiments were conducted in transgenic mouse lines in which the morphology and circuit integration of adult-generated neurons could be manipulated. To this end, we crossed Nestin-Cre$^{ERT2-/+}$ mice (line 4 from [27]), which express tamoxifen (TAM)-inducible Cre recombinase in neural precursor cells in the dentate gyrus (DG), with two other transgenic mouse lines. First, we crossed Nestin-Cre$^{ERT2-/+}$ mice with mice in which the gene encoding semaphorin 5 A (Sema5A) could be conditionally deleted in a Cre-dependent manner (Sema5A$^{f/f}$; a gift from Dr. Roman Giger, University of Michigan [28]). In offspring from this cross expressing both transgenes, TAM treatment results in Sema5A deletion in DG neural precursor cells and their progeny (Sema5A$^{-/-}$ mice). Littermates that did not express Cre in neural precursor cells following TAM treatment, therefore precluding deletion of the Sema5A gene, were used as controls (Sema5A$^{+/+}$ mice). Second, we crossed Nestin-Cre$^{ERT2-/+}$ mice with transgenic mice expressing a lox-P STOP cassette upstream of the gene for ChR2-EYFP fusion protein at the Rosa26 locus (ChR2-EYFP mice; JAX:012569). In offspring from this cross expressing both transgenes, TAM treatment results in ChR2-EYFP expression in DG neural precursor cells and their progeny (ChR2^{+} mice). Littermates that did not express Cre in neural precursor cells following TAM treatment, therefore precluding expression of the ChR2-EYFP gene, were used as controls (ChR2^{-} mice). Transgenic mice used in behavioral experiments were C57BL/6 J background. Only male mice were used in the PTSD model experiments, and both sexes were used for the cocaine-conditioned place preference experiments.

In experiments in which we characterized morphology of retrovirus-infected adult-generated neurons, we used male WT or Sema5A$^{f/f}$ mice. To characterize the effects of wheel running on DG neurogenesis, we used male WT mice.

Surgery. Mice were pre-treated with atropine sulfate (0.1 mg/kg, i.p.), anesthetized with chloral hydrate (400 mg/kg, i.p.) or isoflurane (3% induction, 1.0–1.5% maintenance), and administered analgesic meloxicam (4 mg/kg, s.c.). Following placement in a stereotaxic frame, mice were topically administered lidocaine around the incision site. An incision was made in the scalp, and holes were drilled bilaterally above the DG (AP −1.9 mm, ML ± 1.5 mm or AP −2.3 mm, ML ± 1.5 mm from bregma for morphology and behavioral experiments, respectively). For retrovirus delivery, a glass micropipette connected to a Hamilton syringe via tubing and containing virus was lowered to the DG (DV −2.2 mm from bregma), and 0.5 µl virus was injected slowly (0.1 µl/min). Following the injection, the glass micropipette remained in place for 10 min before retraction. The scalp of Sema5A$^{f/f}$ mice was sutured and polysporin was applied to the wound. Mice administered 1.0 ml saline (s.c.) and left to recover on a heating pad before returning to the vivarium.

For mice in the optogenetic stimulation experiments, implants were prefabricated in-house by attaching ~10 mm piece of 200-µm diameter optical fiber (0.39 numerical aperture, Thorlabs, FT200EMT, Newtown, NJ) to a zirconia ferrule (Thorlabs, CFLC230-10) with epoxy resin and polishing both ends of fiber. Optical fibers were lowered into the brain above the DG (DV −1.7 mm or DV −2.0 mm from bregma for morphology and behavioral experiments, respectively) and secured with jeweler screws and black dental cement. Mice administered 1.0 ml saline (s.c.) and left to recover on a heating pad before returning to the vivarium. For ChR2^{+} and ChR2^{-} mice in behavioral experiments, surgery occurred 6–7 d before training. Surgery occurred 2 days before the start of the optogenetic stimulation protocol for WT mice that received microinjections of retrovirus.

Treatments

Tamoxifen (TAM). To induce recombination in the transgenic mouse lines, TAM (Sigma, T5648) was injected. Injectable TAM solution was prepared by dissolving 30 mg TAM in 100 µl ethanol and vortexing, followed by 900 µl sunflower oil. The solution was sonicated until TAM was fully dissolved. Sema5A$^{+/+}$ and Sema5A$^{-/-}$ mice received an i.p. injection of TAM (180 mg/kg) once daily for 5 days, beginning ~24-h after the reminder shock treatment. ChR2^{+} and ChR2^{-} mice received 3 days of TAM treatment, beginning 2–3 days after surgery, to allow sufficient recombination to occur before the start of the optogenetic stimulation protocol.

Retroviruses. To target viral expression to neural precursor cells, retroviruses based on the Moloney murine leukemia virus, which express only in dividing cells [29–31], were used. Genes expressed using retroviruses were driven by the CAG promoter. Specifically, retroviruses were generated using the following plasmids: pCAG-GFP (Addgene #16664, a gift from Dr. Fred Gage), pCAG-GFP-IRES-Cre (Addgene #48201, a gift from Dr. Fred Gage), and pCAG-hChR2(H134R)-EYFP (Addgene #114367, a gift from Mingshan Xue). Viral particles were generated as previously described [32, 33]. Briefly, retroviruses were prepared by transfecting Platinum-gp cells with plasmids containing an amphotrophic envelope (vesicular stomatitis virus-glycoprotein) and the transgenes. Platinum-E cells were then infected to generate a stable virus-producing cell line. The concentrated viral solution was obtained by ultraspeed centrifugation with final titers of ~1.7×10^2–3.5×10^9 units/ml.

Running wheels. Running wheels were placed in the home cage 1–2 d after training. Mice voluntarily ran on the wheels as described previously [14, 17, 34]. Running wheels remained in the cage until the day before testing began (~28 d). Running wheels were not placed in the cages of control (Sedentary) mice.

Optogenetic stimulation. The optogenetic stimulation protocol used to promote morphological development of adult-generated neurons was described previously [34]. Optogenetic stimulation began 1 d after training (ChR2^{+} and ChR2^{-} mice) or 2 d after surgery in the GFP or ChR2-EYFP retrovirus-treated mice. Mice were placed in a clean cage located in a neutral, novel room. The implanted optical fibers were attached to a laser source (Laserglow), which was controlled by a waveform generator (Agilent Technologies). Tethered mice were allowed to freely explore the cage while receiving light stimulation during the daily 11-min sessions. During each session, mice received 3 epochs of 473-nm light stimulation (0.4 mW, 10 Hz, 15-ms pulses) from 60 to 120, 300 to 360, and 540 to 600 s. Following the completion of each session, mice were returned to their home cage. Mice received 14 sessions of optogenetic stimulation.

Behavior

Inhibitory avoidance (IA) task. The IA task was adapted from work previously done using rats [26]. The IA apparatus was a rectangular (25.5 cm × 16.5 cm × 17.7 cm height) shuttle box divided into two compartments separated by a sliding door. The shuttle box was placed inside of a fear conditioning chamber (Med Associates) to deliver the shock stimulus via the shock-grid floor. The apparatus was scented with ethanol sprayed in the drop pan below the shock-grid. The "safe" compartment was white and

illuminated by an overhead light placed inside the larger fear conditioning chamber, and the shock compartment was colored black and covered from outside light sources. On the training day, mice were placed into the white compartment of the shuttle box facing away from the door. After 10 s, the door was manually opened. The door was closed 1 s after mice entered the dark compartment and a single 2-s foot shock (0, 0.5, 1, 2, or 3 mA) was delivered immediately. Following the shock, mice remained in the dark compartment for 10 s, then were returned to their home cage. For experiments in which reminder shocks were delivered, mice were placed in a novel fear conditioning chamber located in a separate room and immediately given a 2-s reminder shock (1 or 3 mA), 1 or 28 d after training. Mice were returned to their home cage within <10 s of the reminder shock.

IA testing occurred in one of two settings, referred to as Context A and Context B beginning 1-30 d after IA training. Context A was the identical to the apparatus used for training. For extinction and testing sessions, mice were returned to the white compartment of the Context A shuttle box and the door was manually opened after 10 s. The latency for the mice to enter the dark compartment was recorded. No shocks were delivered during these sessions. For extinction sessions, mice remained in the dark compartment of the shuttle box for 5 min before removal. Otherwise, mice were removed 10 s after entry into the dark compartment of Context A. Generalization was tested in Context B, which was modified using plastic inserts. The walls of the Context B apparatus were rounded and colored off-white and navy. The off-white compartment was illuminated by an overhead light, and Context B was not scented with ethanol. Mice were tested identically in Context B as in Context A.

Open field exploration. To assess anxiety-like behavior, mice were placed in an open field arena (45 cm × 45 cm × 20 cm height) and allowed to explore for 10 min. The behavior of the mice was recorded by an overhead camera and Limelight 2 software (Actimetrics). The percentage of time mice spent in the center (15 cm × 15 cm) versus periphery of the apparatus was reported. Additionally, quantified overall exploration of open field environment by computing an entropy measure. For the entropy analysis, mouse position within the open field arena was tracked using custom Python scripts. Briefly, the location of the mouse was determined by comparing the behavior recording to a reference image of the empty apparatus. Using the position data, a probability distribution for mouse position over all pixels of the arena was calculated and smoothed with a Gaussian filter. Entropy of this probability distribution was calculated using the entropy function from the SciPy Python package.

Conditioned place preference (CPP) task. CPP was performed as previously described [35]. The CPP apparatus consisted of two 15 cm × 20 cm chambers connected by a guillotine door. One compartment contained white walls and a transparent, rough-textured floor. The opposite compartment contained black-and-white striped walls and a smooth white floor wiped with 0.2 ml of 3% acetic acid solution. The task was separated into three phases: habituation, training, and testing. On the habituation day, mice were placed in one of the compartments and allowed to freely explore both chambers for a total of 10 min. One day later, conditioning began for three consecutive days. On each conditioning day, each morning mice were confined to one chamber for 15 min immediately after an i.p. injection of saline. In the afternoon of each conditioning day, mice were confined to the opposite chamber for 15 min immediately after i.p. injection of cocaine (7.5 mg/kg). Memory for the CPP training was assessed 28 d later during the test session. Drug-free mice were placed into the apparatus and allowed to freely explore both compartments for 10 min. The position of the mice was monitored by overhead cameras and analyzed using Limelight 2 software (Actimetrics). The CPP score for each mouse during the test session was calculated as [time spent in cocaine-paired compartment – time spent in saline-paired compartment].

Histology

Perfusion. Mice were perfused after the completion of the behavioral protocols, or 30 d after retrovirus microinjections. Mice were deeply anesthetized with chloral hydrate and transcardially perfused with ice-cold phosphate-buffered saline (PBS) followed by 4% paraformaldehyde (PFA). Brains were extracted and post-fixed overnight in 4% PFA then transferred to 30% sucrose for at least 48 h. Brains were sectioned coronally using a Leica CM1850 cryostat. Tissue sections (50-µm thickness) across the extent of the hippocampus were collected.

Immunohistochemistry. Free-floating sections were washed with PBS and then placed in blocking solution (5% normal goat or donkey serum and 0.3% Triton-X) for 2 h at room temperature. Next, sections were incubated with primary antibodies diluted in the same blocking solution: chicken anti-GFP (1:500, Aves, cat# GFP1020) or goat anti-doublecortin (DCX; 1:500, Santa Cruz, cat# sc-8066) for 72 h at 4 °C. Sections were washed again and then incubated with secondary antibodies diluted in PBS: goat anti-chicken AlexaFluor 488 (1:500, ThermoFisher, cat# A-11039) or donkey anti-goat AlexaFluor 568 (1:500, ThermoFisher, cat# A-11057) for 24 h at 4 °C (for GFP) or 2 h at room temperature (for DCX). Sections were counterstained with DAPI, mounted onto gel-coated slides, and coverslips were sealed with Permafluor mounting medium.

Neurogenesis quantification. We quantified neurogenesis in two ways. First, to measure the number of immature neurons in the DG we counted DCX in the DG following wheel running, Sema5A deletion, or optogenetic stimulation. Images were captured using a LSM710 confocal microscope (Zeiss) using a 40×/1.3 NA objective. Z-stacks (1-µm interval) through the upper blade of the DG were taken from 3–6 tissue sections per mouse. The number of DCX^+ cells was counted manually in FIJI and reported per volume of DG granule layer (DCX^+ cells/mm^3). Next, to assess survival of adult-generated neurons we counted GFP^+ DG neurons 30-d post retrovirus microinjection. GFP^+ neurons were counted manually using a 40× objective on an epifluorescent microscope. The total number of GFP^+ neurons per DG was estimated by counting the total neurons in 1/6 of tissue sections and multiplying the obtained value by 6 (GFP^+ cells/DG).

Morphological analyses. Images were captured using a LSM710 confocal microscope (Zeiss). For dendritic length analyses, z-stacks (0.5-µm interval) of the DG were captured using a 20× objective. All GFP^+ neurons were traced using the Simple Neurite Tracer plugin for FIJI.

To quantify spine density, we acquired z-stacks (0.5-µm interval) of GFP^+ dendritic processes at the outer molecular layer of the DG using the 40×/1.3 NA objective and the following settings: 0.07 × 0.07 × 1 µm voxel size, 1024 × 1024 pixels, and 3× digital zoom. The number of spines per dendritic segment were counted manually from the maximum z-projection, and spine density was calculated by dividing the obtained value by the length of the dendritic segment.

To quantify large mossy terminal (LMT) density, we acquired z-stacks of GFP^+ LMTs in CA3 using the 40×/1.3 NA objective and the following settings: 0.21 × 0.21 µm voxel size, 1024 × 1024 pixels. Axonal length and the number of LMTs were counted manually from the maximum z-projection, and LMT density was calculated by dividing the obtained value of LMTs by the axonal length.

Statistics

No statistical methods were used to determine sample size, but sample sizes were equivalent to previously published studies [14, 16, 17, 34]. Group sizes are detailed in each figure caption, and

an estimate of variation (standard error of the mean) included in all graphs. For experiments using WT mice, no randomization was used. For experiments using transgenic Nestin-Cre$^{ERT2-/+}$ mice, randomization was not used, but mice in the control group were littermates of mice in the experimental group. For experiments using transgenic mice, experimenters were blinded to genotypes during data collection analysis. Mice in the retrovirus and optogenetic experiments were excluded if they did not show virus expression in the DG and/or if optical fibers were not positioned above the dorsal DG.

We evaluated the normality (Shapiro-Wilk test) and homoscedasticity (Bartlett or Brown-Forsythe test) for all datasets. For datasets that violated parametric assumptions of normality and/or homogeneity of variance, we used Mann-Whitney *U* tests or Krusakal-Wallis ANOVA followed by between-group Mann-Whitney *U* planned comparisons. Otherwise, we used unpaired *t*-tests or parametric one-way or factorial ANOVA (with repeated measures, when appropriate), followed by post-hoc Tukey HSD tests. Critical value α was set to 0.05 or modified using Bonferroni correction, when appropriate.

RESULTS

Establishing the double trauma model for PTSD in mice

The original double trauma paradigm was developed in rats [26], and so we adapted it for use in mice (Fig. 1a). We first assessed the impact of shock intensity on IA learning (event 1). Mice were placed into the light compartment of an IA apparatus, and punished with a footshock (0-3 mA) upon entry into the dark compartment. When subsequently placed back into the light compartment of the apparatus on the following day, mice took longer to enter the dark compartment compared to non-shocked controls (Fig. 1b). Similar to rats [26], however, latencies did not increase proportionally with shock intensity. Rather, retention latencies followed an inverted U-shaped function, with latencies in the 3 mA condition lower than those in the 2 mA condition. The next day mice were placed in the light compartment of a distinct training IA apparatus (context B), and the time for mice to enter the dark compartment was recorded. In this distinct apparatus, latencies increased as a function of training shock intensity. However, overall they were much lower than those in the original training context, indicating only mild levels of generalization between these two contexts (Fig. 1c). In rats, only the higher shock intensity led to the emergence of PTSD-like behavioral phenotypes [26]. Therefore, in all subsequent experiments, mice received IA training with the 3 mA footshock.

We next assessed the impact of a low or high intensity reminder footshock (i.e., event 2) on the emergence of PTSD phenotypes such as threat generalization, extinction deficits and anxiety-like behaviors. In the first experiment, all mice were trained in IA (day 1), tested in the IA apparatus (day 3) and then given either a low (1 mA) or high (3 mA) intensity reminder footshock on day 4. IA memory was then assessed in the training apparatus (context A; day 5) and in a distinct apparatus (context B; day 6) in order to assess generalization (Fig. 1d). In context A, latencies to enter the dark compartment were elevated in the high intensity (but not low intensity) reminder shock group, approaching the 900 s cut-off (Fig. 1e). In context B, latencies to enter the dark compartment were elevated in the high intensity group (Fig. 1f). Similar to rats [26], these results suggest that a highly stressful reminder of the initial traumatic experience reinstates normal memory expression and this generalizes to other contexts.

In separate cohorts of mice, we assessed whether the high intensity footshock would additionally induce anxiety-like behaviors and extinction deficits. In the open field (Fig. 1g), mice treated with the high intensity reminder shock spent less time exploring the central zone compared to mice receiving the low intensity reminder shock (Fig. 1h). Consistent with this, spatial entropy (reflecting the extent to which mice search the entire open field arena) was reduced in the high intensity reminder shock group relative to naïve controls (Fig. 1i). To examine extinction, mice were placed into the light compartment of the IA apparatus on 5 consecutive days (days 3-7), and the latency to enter the compartment was recorded (Fig. 1m). Extinction was slowed in mice treated with the high intensity shock. Following extinction training, enhanced fear reinstatement was observed in the high intensity shock group (day 9; Fig. 1n).

Similar to rats, these data indicate that a highly stressful reminder of the initial traumatic experience reinstates the original trauma memory, and induces threat generalization, anxiety-like behavior and extinction deficits.

PTSD-like symptoms persist at remote delays in the double trauma paradigm

Because new neurons take 2–3 weeks to synaptically integrate into hippocampal circuits [4, 5], the impact of manipulations of hippocampal neurogenesis on forgetting are delayed, and not immediately apparent [34]. Therefore, we next adapted the double trauma PTSD paradigm to examine behavior at remote delays (with respect to initial IA training or event 1) to allow sufficient time for neurogenesis-mediated remodeling of hippocampal circuits.

In the first series of experiments, events 1 and 2 occurred close together in time. Specifically, mice were trained in IA (day 1) and received either a low (1 mA) or high (3 mA) intensity reminder shock on day 2. Four weeks later IA was assessed in the original training apparatus (context A; day 30) and in the distinct apparatus (context B; day 31) in order to evaluate generalization. In context A, latencies to enter the dark compartment were elevated, but did not differ between the low and high reminder shock groups (Fig. 2b). However, in context B, the high reminder shock mice took longer to enter the dark compartment (Fig. 2c), indicating that the high intensity shock produced greater levels of generalization. In the open field, mice treated with the reminder shock spent less time exploring the central zone compared to naïve mice (Fig. 2d). Consistent with this, spatial entropy was reduced in the reminder shock groups relative to naïve controls (Fig. 2e). In a separate cohort of mice, we examined extinction (Fig. 2f). Compared to mice receiving the weak reminder shock, extinction was slowed in mice treated with the high intensity shock. Following extinction training, enhanced fear reinstatement was observed in the high intensity shock group (Fig. 2g).

In the second series of experiments, events 1 and 2 were separated by 4 weeks. Specifically, mice were trained in IA (day 1) and received either a low (1 mA) or high (3 mA) intensity reminder shock 4 weeks later (day 29). IA was assessed in the original training apparatus (context A; day 30) and in the distinct apparatus (context B; day 31) in order to evaluate generalization (Fig. 2h). In context A, latencies to enter the dark compartment were elevated in both groups. However, mice that received the high intensity reminder shock took longer to enter the dark compartment (Fig. 2i). Similarly, in context B, mice that received the high intensity reminder shock took longer to enter the dark compartment (Fig. 2j), indicating that the high intensity shock produced greater levels of generalization. In the open field (Fig. 2k, l), mice treated with both of high and low intensity reminder shock spent less time exploring the central zone and exhibited decreased entropy compared to naïve controls. In a different cohort of mice, extinction was assessed (Fig. 2m). Extinction was slowed in mice in the high intensity shock group, with these mice exhibiting longer latencies to enter the dark compartment compared to mice in the low intensity group. Moreover, at the completion of extinction training a reminder shock reinstated fear in the high, but not low, intensity group (Fig. 2n).

Together, these two experiments indicate that the double trauma PTSD paradigm produces lasting effects on behavior. Regardless of whether events 1 and 2 occur close together or far

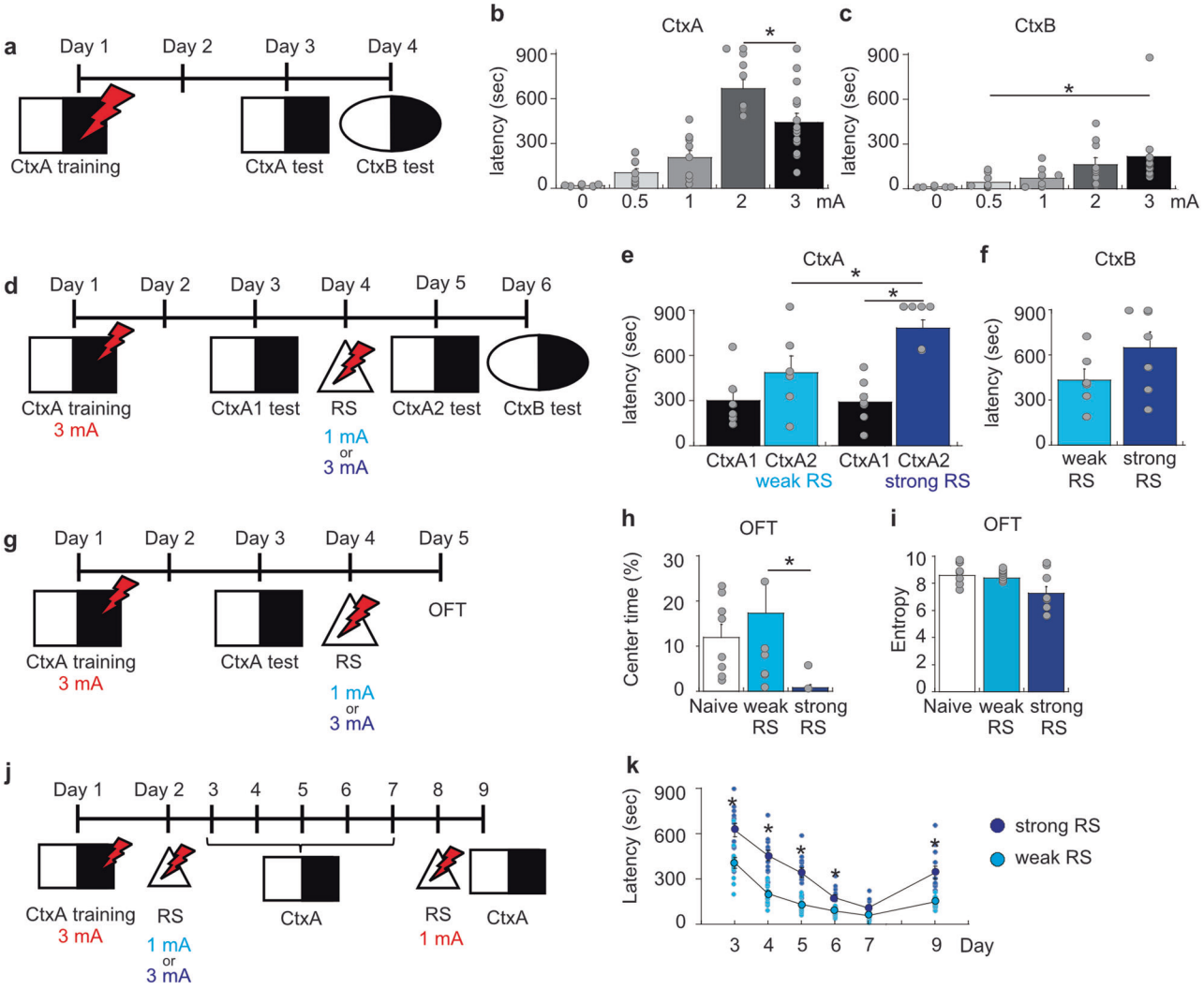

Fig. 1 Development of a double trauma model for PTSD in mice. a Experimental schedule for memory retention tests against a single 2 s foot shock. The time to enter the dark compartment was recorded. **b** The latency in Context A (CtxA) shows inverted U-shape in response to a single foot shock (0, 0.5, 1, 2, or 3 mA) (Kruskal-Wallis test, $H_4 = 40.82$, $P < 0.0001$; *Mann-Whitney U planned comparisons: 2 mA versus 3 mA, $U = 30$, $P = 0.019$). **c** The latency in CtxB, which was different in wall shape and smell compared to CtxA, increased depends on shock intensity (Kruskal-Wallis test, $H_4 = 33.31$, $P < 0.0001$; Mann-Whitney U planned comparisons (corrected $\alpha = 0.016$): 0.5 mA versus 3 mA, $U = 6$, $P < 0.0001$; 1 mA versus 3 mA, $U = 30$, $P = 0.019$; 2 mA versus 3 mA, $U = 50$, $P = 0.26$). **d** The latency was tested as CtxA1 after the 3-mA foot shock in CtxA, and CtxA2 and CtxB after the reminder foot shocks (RS; weak 1 mA or strong 3 mA) in a different context. **e** A strong reminder shock of 3 mA increased the latency in CtxA (Repeated measures ANOVA, Reminder × Day interaction: $F_{1,11} = 7.46$, $P = 0.020$). **f** A strong reminder shock of 3 mA modestly increased the latency in CtxB compared to a weak reminder shock of 1 mA (Unpaired t-test, $t_{11} = 1.60$, $P = 0.13$). **g** Anxiety-like behavior in the open field test (OFT) was assessed one day after the reminder shock s. **h** A strong reminder shock of 3 mA decreased center time (%) compared with a weak reminder shock of 1 mA (Kruskal-Wallis test, $H_2 = 13$, $P = 0.0016$; Mann-Whitney U planned comparisons: 1 mA versus 3 mA, $U = 3$, $P = 0.0009$. **i** Entropy did not differ across reminder shock groups (Kruskal-Wallis test, $H_2 = 4.4$, $P = 0.11$). **j** Experimental schedule for memory extinction from one day after the reminder shock (1 mA or 3 mA). A reminder shock of low intensity (1 mA) was administrated after extinction to assess memory reinstatement (on day 9). **k** The strong reminder shock group showed slower extinction (context A; day 3–7) and high level of memory reinstatement (context A; day 9) (Mann-Whitney U planned comparisons for 1 mA versus 3 mA (corrected $\alpha = 0.0083$): Day 3, $U = 18$, $P = 0.0011$; Day 4, $U = 2$, $P < 0.0001$; Day 5, $U = 5$, $P < 0.0001$; Day 6, $U = 17$, $P = 0.0009$; Day 7, $U = 30$, $P = 0.015$; Day 9, $U = 9.5$, $P < 0.0001$). Data are represented as mean ± S.E.M. Data points represent individual mice (**b**, **c**: 3 mA, n = 14 mice, other groups, n = 10 mice; **e**, **f**: 3–1 mA, n = 6 mice, 3–3 mA, n = 7 mice; **h**, **i**; n = 8 mice for each group; **k**: n = 12 mice for each group). Statistical significance is indicated by asterisks.

apart in time, elevated threat generalization and deficient extinction was evident at remote time points (relative to initial IA training or event 1). In contrast with the recent time point, no differences in open field behavior were observed in mice that received the high and low intensity reminder shock.

Post-training exercise weakens IA memory and attenuates PTSD-like behaviors

Exercise-induced increases in neurogenesis following training induce forgetting of contextual and spatial memories that depend on the hippocampus [14–19, 21, 22, 36]. We next tested whether post-training exercise would similarly induce forgetting in the double trauma PTSD paradigm, weakening IA memories and preventing the emergence of extinction deficits, generalization, and anxiety-like behaviors.

In the first series of experiments, we examined the impact of exercise *following* both IA training and the reminder shock (i.e., following the second traumatic event). In these experiments, all mice were trained in IA (day 1), given a reminder shock in a different context (day 2) and then housed with (Running group) or

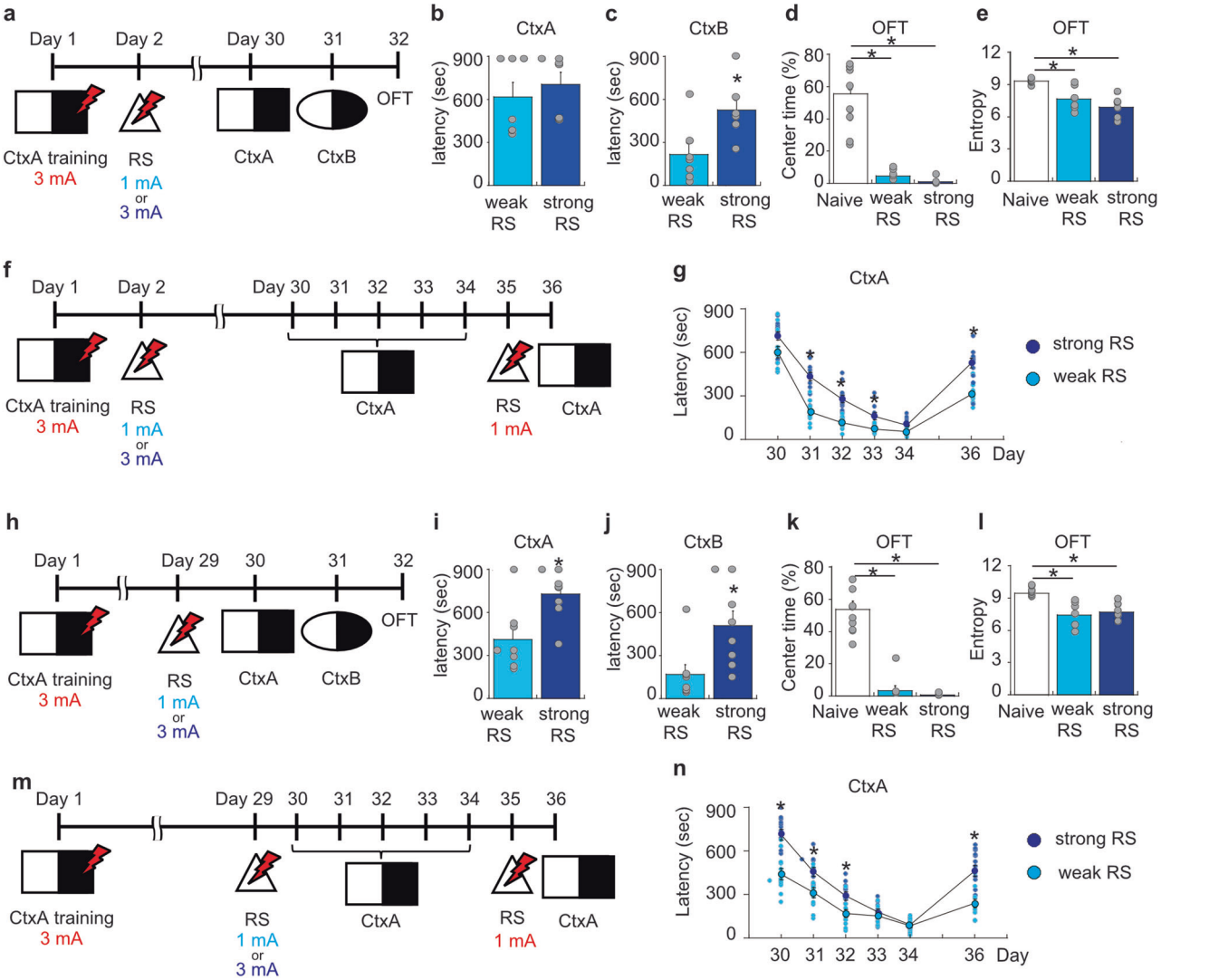

Fig. 2 PTSD-like symptoms persist at remote delays. a A reminder shock was administered 1 day after the training in Context A (CtxA), and latency was tested 4 weeks later. **b** No difference in CtxA latency 4 weeks after a reminder shock (Mann-Whitney *U*-test, $U = 19$, $P = 0.53$). **c** High intensity (3 mA) reminder shock group mice showed increased latency in CtxB (Unpaired *t*-test, $t_{12} = 2.85$, $P = 0.015$). **d** Center time (%) in the open field test was decreased in both of shock groups than no shock group (Kruskal-Wallis test, $H_2 = 18$, $P = 0.00013$; Mann-Whitney *U* planned comparisons (corrected $\alpha = 0.016$): Naïve versus 1 mA, $U = 0$, $P = 0.0001$; Naïve versus 3 mA, $U = 0$, $P = 0.0001$; 1 mA versus 3 mA, $U = 12$, $P = 0.11$). **e** The groups that received foot shocks exhibited decreased entropy compared with no shock group (Kruskal-Wallis test, $H_2 = 16$, $P = 0.00032$; Mann-Whitney *U* planned comparisons (corrected $\alpha = 0.016$): Naïve versus 1 mA, $U = 3$, $P = 0.0007$; Naïve versus 3 mA, $U = 0$, $P = 0.0001$; 1 mA versus 3 mA, $U = 15$, $P = 0.26$). **f** Experimental schedule for memory extinction 4 weeks after the reminder shock (1 mA or 3 mA). A reminder shock of low intensity (1 mA) was administrated after extinction to assess memory reinstatement in CtxA test on day 36. **g** High intensity reminder shock group showed slower extinction (context A; day 30–34) and high level of memory enhancement (context A; day 36) (Mann-Whitney *U* planned comparisons for 1 mA versus 3 mA (corrected $\alpha = 0.0083$): Day 30, $U = 39$, $P = 0.060$; Day 31, $U = 3$, $P < 0.0001$; Day 32, $U = 2$, $P < 0.0001$; Day 33, $U = 25.5$, $P = 0.0058$; Day 34, $U = 28$, $P = 0.0096$; Day 36, $U = 11$, $P = 0.0001$). **h** A reminder shock and extinction training were administrated 4 weeks after the training in CtxA, and memory reinstatement was tested in CtxA on day 36 following a low intensity (1 mA) reminder shock. **i, j** High intensity reminder shock group showed increased latency in CtxA and CtxB (Mann-Whitney *U*-tests: **i**, $U = 9$, $P = 0.014$; **j**, $U = 7$, $P < 0.0068$). **k** Center time (%) in the open field test was decreased in both of shock groups compared with no shock group (Kruskal-Wallis test, $H_2 = 19$, $P < 0.0001$; Mann-Whitney *U* planned comparisons (corrected $\alpha = 0.016$): Naïve versus 1 mA, $U = 0$, $P < 0.0001$; Naïve versus 3 mA, $U = 0$, $P < 0.0001$; 1 mA versus 3 mA, $U = 32$, $P = 0.99$). **l** The groups that received foot shocks decreased entropy compared to no shock group (Kruskal-Wallis test, $H_2 = 16$, $P = 0.00040$; Mann-Whitney *U* planned comparisons (corrected $\alpha = 0.016$): Naïve versus 1 mA, $U = 0$, $P = 0.0002$; Naïve versus 3 mA, $U = 0$, $P = 0.0002$; 1 mA versus 3 mA, $U = 17$, $P = 0.94$). **m** Experimental schedule for memory extinction 1 day after the reminder shock (1 mA or 3 mA). Reminder shock of low intensity (1 mA) was administrated after extinction to assess memory reinstatement in CtxA test on day 36. **n** High intensity reminder shock group showed longer latency and memory enhancement compared to lower intensity group (Mann-Whitney *U* planned comparisons for 1 mA versus 3 mA (corrected $\alpha = 0.0083$): Day 30, $U = 10$, $P = 0.0001$; Day 31, $U = 16$, $P = 0.0006$; Day 32, $U = 17$, $P = 0.0009$; Day 33, $U = 46$, $P = 0.14$; Day 34, $U = 54$, $P = 0.32$; Day 36, $U = 6$, $P < 0.0001$). Data are represented as mean ± S.E.M. Data points represent individual mice (**b**, **c**: n = 7 mice for each group; **d**, **e**: 0 mA, n = 10 mice, other groups, n = 7 mice for each group; **g**: n = 10 mice for each group; **i**, **j**: n = 8 mice for each group; **k**: n = 10 mice, other groups, n = 8 mice for each group; **l**: 0 mA, n = 10 mice, other groups, n = 6 mice for each group; **n**: n = 12 mice for each group). Statistical significances are indicated by asterisks.

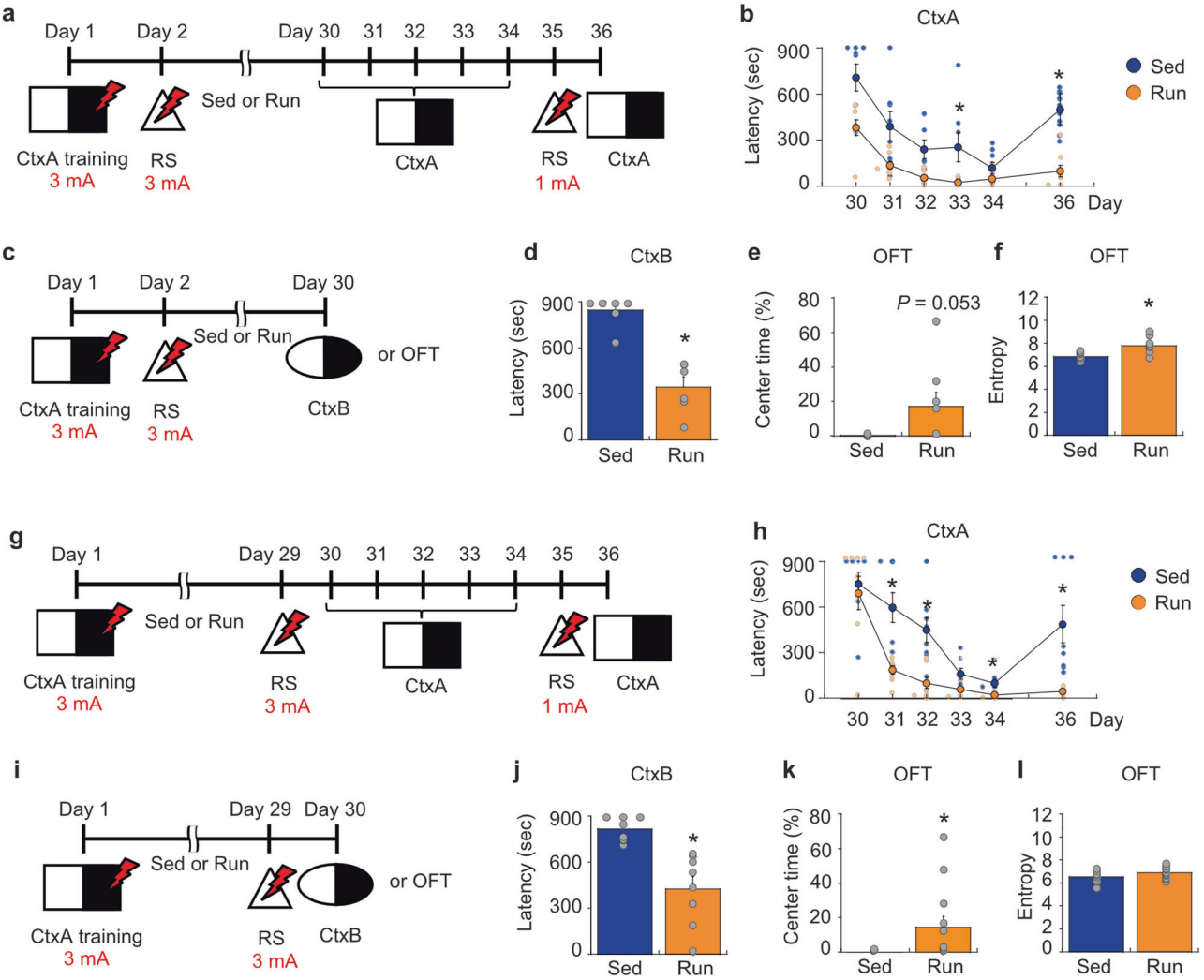

Fig. 3 Exercise attenuates PTSD-like phenotypes. a Experimental schedule of CtxA memory extinction and reinstatement to test the effect of exercise after the reminder shock. CtxA memory was tested on five consecutive days from day 30, and reinstatement was tested 1 day after a reminder shock. **b** Post-training exercise weakened CtxA memory and memory reinstatement following a 1 mA reminder shock (Mann-Whitney *U* planned comparisons for Sedentary versus Running (corrected $\alpha = 0.0083$): Day 30, $U = 11$, $P = 0.028$; Day 31, $U = 11$, $P = 0.026$; Day 32, $U = 8$, $P = 0.010$; Day 33, $U = 4$, $P = 0.0019$; Day 34, $U = 16.5$, $P = 0.11$; Day 36, $U = 5$, $P = 0.0030$). **c** Generalization in CtxB or anxiety-like behavior in open field test (OFT) were assessed in CtxB test 4 weeks after the reminder shock. **d** Running suppressed the latency in CtxB (Mann-Whitney *U*-test, $U = 0$, $P = 0.0022$). **e** Excercise modestly increased the center time (%) in the OFT (Mann-Whitney *U*-test, $U = 14$, $P = 0.053$). **f** Exercise increased entropy in the OFT (Unpaired *t*-test, $t_{14} = 3.34$, $P = 0.0048$). **g** Experimental schedule of CtxA memory extinction and reinstatement to assess the effect of exercise before the reminder shock. **h** The running group showed rapid extinction and suppressed reinstatement (Mann-Whitney *U* planned comparisons for Sedentary versus Running (corrected $\alpha = 0.0083$): Day 30, $U = 31$, $P = 0.95$; Day 31, $U = 3$, $P = 0.0011$; Day 32, $U = 2$, $P = 0.0006$; Day 33, $U = 10$, $P = 0.020$; Day 34, $U = 4$, $P = 0.0017$; Day 36, $U = 0$, $P = 0.0002$). **i** Generalization or anxiety-like behavior was tested one day after the reminder shock, which was administered 4 weeks after the CtxA training. **j** Exercise suppressed the latency in CtxB (Mann-Whitney *U*-test, $U = 0$, $P = 0.0002$). **k** Exercise increased center time (%) in the OFT (Mann-Whitney *U*-test, $U = 21$, $P = 0.0053$). **l** Exercise did not affect entropy in the OFT (Unpaired *t*-test, $t_{20} = 1.76$, $P = 0.094$). Data are represented as mean ± S.E.M. Data points represent individual mice (**b**: n = 8 mice for each group; **d**: n = 6 mice for each group; **e**, **f**: n = 8 mice for each group; **h**, **j**: n = 8 mice for each group; **k**, **l**: Sed, n = 10 mice, Run, n = 12 mice). Statistical significance is indicated by asterisks.

without (Sedentary group) a running wheel for the next 4 weeks. Extinction deficits, threat generalization, and anxiety-like behaviors were then examined in separate groups of mice.

To examine extinction, mice were subsequently placed into the lighted compartment of the IA apparatus on 5 consecutive days (Fig. 3a). On the first day of this extinction training (day 30), latencies to enter the dark compartment were lower in the exercise compared to sedentary group, indicating that post-training exercise weakened IA memory. Over the course of extinction training (days 30–34), latencies decreased in both groups, but were consistently lower in the exercise mice. Reinstatement of fear only occurred in the sedentary group. Following a reminder shock, whereas latencies rebounded in the sedentary mice, latencies remained low in the exercise mice (Fig. 3b).

To evaluate threat generalization, a separate cohort of mice were placed in the lighted compartment of an otherwise distinct IA apparatus (context B) on day 30, and the latency to enter the dark compartment was recorded (Fig. 3c). In sedentary mice, latencies to enter the dark compartment were elevated (and were close to the 900 s cut-off), indicating that these mice generalized from the training apparatus (context A) to this distinct apparatus (context B). In contrast, latencies to enter the dark compartment in context B were reduced in mice that exercised post-training, indicating that exercise attenuated generalization (Fig. 3d).

To evaluate anxiety-related behaviors, another cohort of mice were placed in the open field on day 30, and exploratory activity was recorded (Fig. 3c). Compared to the sedentary mice, mice in the exercise group spent more time exploring the central zone of the apparatus (Fig. 3e). Moreover, the exercise mice explored the open field more comprehensively, as reflected by increased spatial entropy compared with sedentary controls (Fig. 3f). Together, these data suggest that exercise following training reduced anxiety-like behavior in the double trauma paradigm.

In the second series of experiments, we examined the impact of exercise following IA training, but *before* the reminder shock. Because the reminder shock is necessary for the emergence of deficient extinction, threat generalization and anxiety-like behaviors, this approach asks whether exercise might work prophylactically to prevent the development of PTSD-like behaviors.

In these experiments, mice were trained in IA (day 1), then housed with (Running group) or without (Sedentary group) a running wheel for the next 4 weeks, and given a reminder shock on day 29. As before, extinction, generalization, and anxiety-like behaviors were then examined in separate cohorts of mice.

In the extinction experiment (Fig. 3g), latencies to enter the dark compartment were similar in the exercise and sedentary group on the first day of extinction training (day 30). However, over the course of extinction training (days 30-34), latencies decreased more steeply in the exercise mice, indicating that exercise accelerated extinction. Moreover, a reminder shock reinstated fear (increased latencies) in the sedentary, but not the exercise, mice (Fig. 3h).

In the threat generalization experiment, mice were placed in the lighted compartment of an otherwise distinct IA apparatus (context B) on day 30 (Fig. 3i), and the latency to enter the dark compartment was recorded. Latencies to enter the dark compartment were reduced in exercise mice (relative to sedentary mice), indicating that exercise prevented the emergence of generalization (Fig. 3j).

To evaluate anxiety-related behaviors, mice were placed in the open field on day 30, and exploratory activity was recorded (Fig. 3i). Compared to the sedentary mice, mice in the exercise group spent more time exploring the central portion of the apparatus (Fig. 3k). Spatial entropy was similar in the exercise and sedentary control groups (Fig. 3l).

In subsets of mice from these experiments, we confirmed that exercise increased hippocampal neurogenesis by staining for the immature neuronal marker, DCX. As we have seen in our previous studies [14, 16, 17], exercise led to an approximate 3-fold increase in DCX^+ cells (Supplementary Fig. 1). These data, therefore, suggest that exercise-induced increases in hippocampal neurogenesis are associated with positive outcomes in the double trauma PTSD paradigm. More specifically, exercise after either the first, or the second, trauma attenuated the emergence of deficient extinction, threat generalization, and anxiety-like behaviors.

Post-training elevation of hippocampal neurogenesis induces forgetting of IA memory and reduces PTSD-like behaviors

While interventions such as voluntary exercise have translational value for treatment of PTSD [37–42], exercise induces several neural and physiological changes other than increasing hippocampal neurogenesis [43]. Therefore, it is unclear whether effects of exercise on PTSD-like behaviors in this mouse model are mediated via neurogenic or non-neurogenic mechanisms. To address this, we next examined the impact of more targeted manipulations of hippocampal neurogenesis on PTSD-related behaviors.

These experiments built on two approaches developed for selectively manipulating hippocampal neurogenesis in adult mice [34]. In the first approach, we expressed the excitatory opsin, ChR2, in neural progenitor cells ($nestin^+$ cells) and their progeny. Photo-activation of these ChR2-tagged cells accelerated their morphological maturation (without affecting their survival) and, when this occurred after training, induced forgetting of contextual fear memories [34].

Adopting an identical approach here, we first confirmed that photo-activation of newly-generated neurons accelerates their morphological maturation and integration into hippocampal circuits. To do this, a retrovirus expressing a tagged, excitatory opsin ChR2-GFP (ChR2 fused to GFP) or control virus (GFP only) was injected into the dorsal dentate gyrus of adult wild-type (WT) mice, and optical fibers were implanted bilaterally above the injection site. Starting 2 days later, mice received daily photo-stimulation (3 × 1 min at 10 Hz) for 15 days. Fifteen days following completion of photo-stimulation, numerous infected granule cells were identified in the innermost layers of the granule cell layer in the dentate gyrus (Supplementary Fig. 2a). Compared to GFP-infected neurons, ChR2-expressing neurons exhibited increased total dendrite length (Supplementary Fig. 2b), spine density (Supplementary Fig. 2c) and LMT density in CA3 (Supplementary Fig. 2d). Similar numbers of control (GFP) and ChR2-expressing infected granule cells were identified (Supplementary Fig. 2e) along with similar levels of DCX-expressing neurons (Supplementary Fig. 2f), confirming that activation did not alter survival rates of infected adult-generated granule cells or increase neurogenesis. Consistent with our previous work, these data indicate that photo-activation of adult-generated granule cells accelerates their integration into hippocampal circuits, without affecting their survival [34].

We next tested whether inducing hyper-integration of adult-generated granule cells would impact the emergence of PTSD-like behaviors in the double trauma paradigm. To do this we crossed nestin-CreERT2 mice with mice that express ChR2 in a Cre-recombinase dependent manner. In adult offspring of this cross expressing both transgenes ($ChR2^+$ mice), tamoxifen (TAM) treatment induces excision of a STOP codon and ChR2 expression in $nestin^+$ cells and their progeny. Offspring that lacked the nestin-CreERT2 transgene served as controls ($ChR2^-$ mice). $ChR2^+$ and $ChR2^-$ mice were treated with TAM on the 3 d that preceded training. Following training and a reminder shock, mice received 14 days of photo-stimulation. Starting day 30, we assessed IA memory, threat generalization and anxiety-like behaviors in the same cohort of mice (Fig. 4a).

Optogenetic stimulation of newly-generated granule cells weakened IA memory, with latency to enter the dark compartment in the training apparatus (context A) reduced in $ChR2^+$ compared to $ChR2^-$ mice (Fig. 4b). When placed in the distinct apparatus (context B), the latency to enter the dark compartment was reduced in $ChR2^+$ compared to $ChR2^-$ mice (Fig. 4c), indicating that threat generalization was reduced by the earlier stimulation of newly-generated neurons. In the open field test, the results were less clear. While $ChR2^+$ mice exhibited a modest increase in overall exploratory behavior (increased spatial entropy), there was no difference in time spent in the central zone between $ChR2^+$ and $ChR2^-$ mice (Fig. 4d, e). Since center time is a more commonly used indicator of anxiety-like behavior, these results suggest that the anxiolytic effects of optogenetic stimulation of newly-generated neurons are less pronounced compared to exercise.

In the second approach, we previously found that conditional deletion of semaphorin 5A (Sema5A) from neural progenitor cells and their progeny increased input and output connectivity of newly-generated neurons, and, when this happened post-training, induced forgetting of contextual fear memories [28, 34]. We first confirmed that conditional Sema5A deletion produces hyper-integration of adult-generated granule cells. In floxed Sema5A mice (Sema5Af/f) we injected retroviruses expressing either GFP alone (retro-GFP) or Cre-recombinase and GFP (retro-cre) into the dentate gyrus and, 30 days later, compared morphology of control

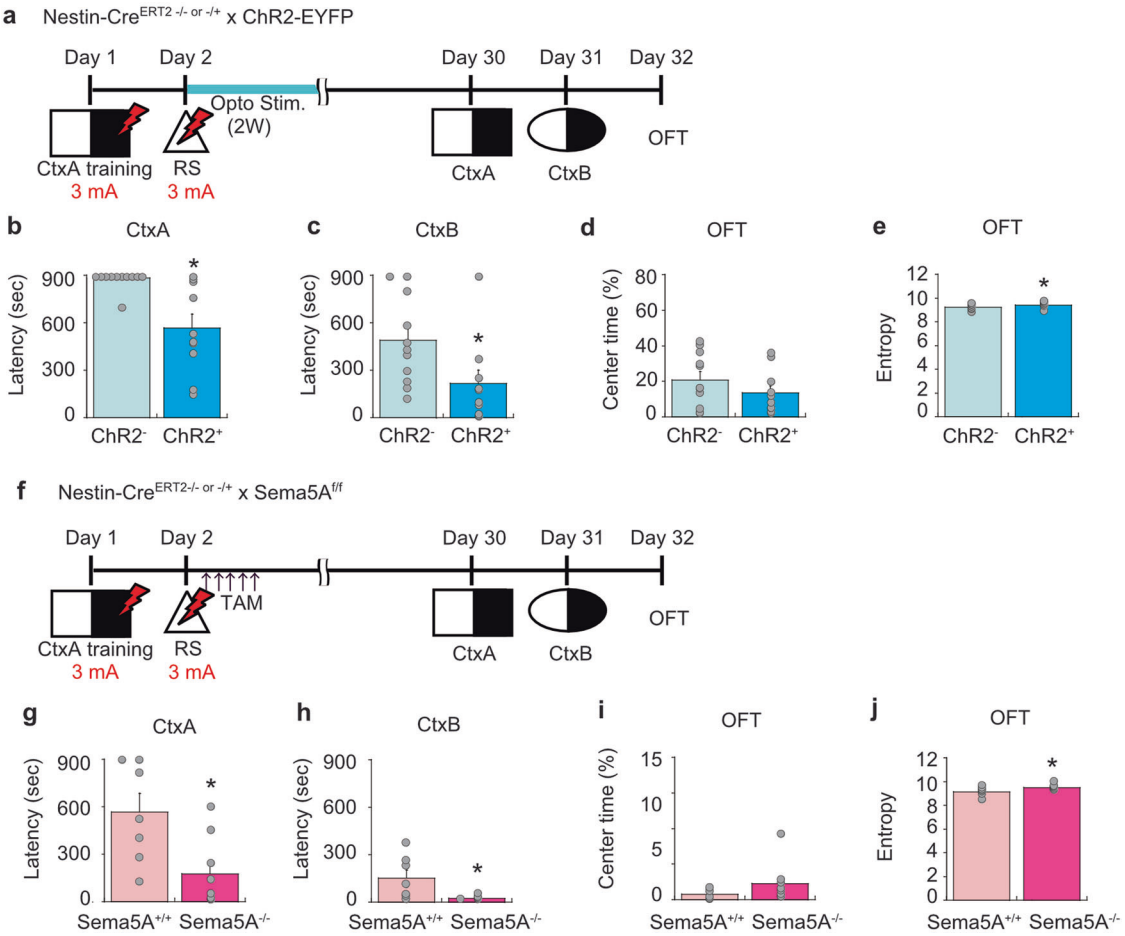

Fig. 4 Hyper-integration of adult-generated granule cells weakens PTSD-like behaviors. a Mice expressed ChR2-eYFP (ChR2$^+$) or control (ChR2$^-$) in nestin positive cells received photo-stimulation (3 × 1 min/day at 10 Hz) for 14 days. Neuronal re-organization was induced by optogenetic stimulation in ChR2$^+$ mice after foot shock administration. ChR2$^-$ control mice also receive foot shocks and photo-stimulation. **b**, **c** ChR2$^+$ mice showed decreased CtxA and CtxB latency 4 weeks after the foot shocks compared to ChR2$^-$ control (Mann-Whitney *U*-tests: **b**, $U = 9$, $P = 0.0002$; **c**, $U = 19$, $P = 0.010$). **d** No difference in center time (%) of the open field test between ChR2$^+$ and ChR2$^-$ mice (Mann-Whitney *U*-test, $U = 40$, $P = 0.31$). **e** ChR2$^+$ mice tended to increase spatial entropy than ChR2$^-$ mice (Mann-Whitney *U*-test, $U = 23$, $P = 0.024$). **f** Sema5A deletion was induced by tamoxifen injection in Sema5A$^{-/-}$ mice. Neuronal re-organization was induced by tamoxifen injection after reminder foot shock in Sema5A$^{-/-}$ mice. The latency in CtxA and CtxB was decreased in the Sema5A deletion group (Mann-Whitney *U*-tests: (**g**) $U = 9$, $P = 0.016$; (**h**) $U = 11$, $P = 0.029$. (**i**) No difference in center time (%) in the open field test between control and Sema5A$^{-/-}$ mice (Mann-Whitney *U*-test, $U = 14$, $P = 0.071$). **j** Sema5A deletion increased spatial entropy in the open-field test (Unpaired *t*-test, $t14 = 2.57$, $P = 0.022$). Data are represented as mean ± S.E.M. Data points represent individual mice (**b**, **c**, **d**, **e**; ChR2$^-$ mice n = 11, ChR2$^+$ mice n = 10, **g**, **h**, **i**, **j**; Sema5A$^{+/+}$ mice, n = 7, Sema5A$^{-/-}$ mice, n = 9). Statistical significance indicated by asterisks.

vs. Sema5A-deficient granule cells. Infected granule cells were identified in the innermost layers of the granule cell layer in the dentate gyrus (Supplementary Fig. 2g), with no differences in number of surviving neurons or immature neurons (Supplementary Fig. 2k–l), confirming that Sema5A deletion does not affect long-term survival of newly-generated granule cells. However, Sema5A deletion increased total dendrite length (Supplementary Fig. 2h), spine density (Supplementary Fig. 2i), and LMT density (Supplementary Fig. 2j), consistent with our previous findings [34].

We next tested whether hyper-integration of adult-generated granule cells following Sema5A deletion would be sufficient to prevent the emergence of PTSD-like behaviors in the double trauma paradigm. To do this, we crossed Sema5A$^{f/f}$ mice with nestin-creERT2 mice. Adult offspring from this cross expressing both transgenes treated with TAM to induce deletion of Sema5A from nestin$^+$ cells (Sema5A$^{-/-}$ mice), or similarly treated littermate controls lacking the nestin-CreERT2 transgene (Sema5A$^{+/+}$ mice), were trained in IA (day 1) and given a reminder shock (day 2). Starting day 30, IA memory, threat generalization and anxiety-like behaviors were assessed (Fig. 4f).

Sema5A deletion from newly-generated granule cells weakened IA memory, with latency to enter the dark compartment in the training apparatus (context A) reduced in in Sema5A$^{-/-}$ compared to Sema5A$^{+/+}$ mice in the test (Fig. 4g). Similarly, the latency to enter the dark compartment in the distinct apparatus (context B) was reduced in in Sema5A$^{-/-}$ compared to Sema5A$^{+/+}$ mice (Fig. 4h), reflecting reduced threat generalization. In the open field test, there was no difference in time spent in the central zone between Sema5A$^{-/-}$ and Sema5A$^{+/+}$ mice (Fig. 4i). However, Sema5A$^{-/-}$ mice explored the arena more comprehensively (increased spatial entropy)(Fig. 4j). Compared to the exercise intervention, the current results suggest that interventions that induce hyper-integration of newly-generated neurons (without changing overall levels of hippocampal neurogenesis) only weakly modulate anxiety-like behaviors.

Post-training increases in hippocampal neurogenesis weakens conditioned place preference for cocaine

Next we asked whether manipulations of hippocampal neurogenesis would be similarly beneficial in another hypermnesic

condition. Strong associations form between drugs of abuse and the places in which they are consumed, and these associations frequently lead to relapse in human addicts [44]. In rodents drug-place associations can be studied using place preference paradigms [45, 46]. Typically in these paradigms, one side of a two compartment apparatus is consistently paired with a drug of abuse (e.g., cocaine), while the other side is paired with saline. Following training, when placed back into the apparatus with access to both the cocaine-paired and saline-paired sides, mice exhibit a preference for the cocaine-paired side. Here we tested whether post-training manipulations of hippocampal neurogenesis would weaken cocaine place preference.

In the first experiment, we used exercise to elevate hippocampal neurogenesis. Mice were habituated to the apparatus, trained for 3 days, and given home cage access to a running wheel (exercise group) or not (sedentary group) for 4 weeks. Place preference was assessed in a probe test on day 32 (Fig. 5a). In this test, sedentary mice spent more time on the cocaine-paired side compared to the saline-paired side, as expected. In contrast, exercise mice spent equivalent time on the cocaine-paired and saline-paired sides, indicating that post-training exercise weakened this place preference memory (Fig. 5b).

In the second experiment, we used the optogenetic approach to manipulate hippocampal neurogenesis following conditioning. $ChR2^+$ mice and their littermate $ChR2^-$ controls were implanted with optical fibers above the dentate gyrus, habituated to the apparatus, and trained in cocaine CPP. Following training, mice received photo-stimulation daily for 14 days, and place preference was assessed in a probe test on day 32 (Fig. 5c). In this probe test, control $ChR2^-$ mice spent more time on the cocaine-paired side compared to the saline-paired side, as expected. In contrast, $ChR2^+$ mice spent less time on the cocaine-paired side, indicating that post-training exercise weakened this cocaine place preference memory (Fig. 5d).

Finally, we tested the effects of hyper-integration of adult-generated granule cells following Sema5A deletion. After the CPP training, $Sema5A^{-/-}$ mice and littermate $Sema5A^{+/+}$ controls were treated with TAM and then assessed in a probe test on day 32 (Fig. 5e). Sema5A deletion decreased time spent in cocaine-paired side compared with controls, indicating hyper-integration of adult-generated granule cells weakened cocaine place preference memory (Fig. 5f).

DISCUSSION

Using the double trauma paradigm to model PTSD, here we showed that elevating hippocampal neurogenesis attenuated PTSD-related behavioral phenotypes in mice. In this paradigm, consecutive traumatic experiences lead to a constellation of behavioral phenotypes associated with PTSD including deficient extinction, threat generalization and anxiety-like behavior. Post-training elevation of hippocampal neurogenesis weakened the original trauma memory, and blunted the associated deficient extinction, threat generalization, and anxiety-like phenotypes. These beneficial effects were observed using a range of interventions to manipulate hippocampal neurogenesis, including voluntary exercise and more neurogenesis-specific interventions that promote hyper-integration of new neurons into hippocampal

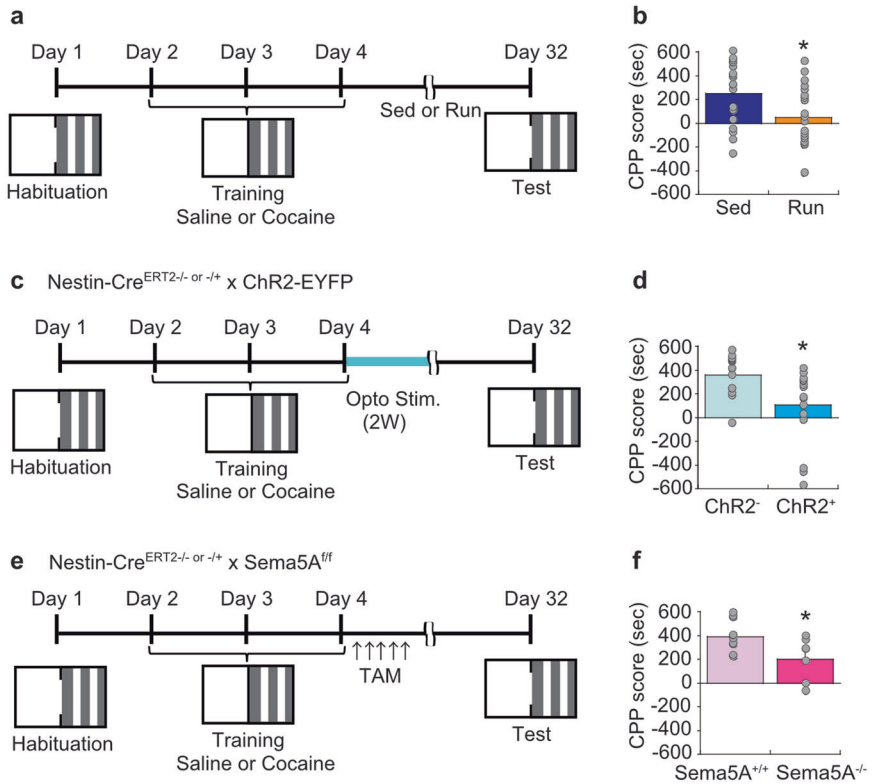

Fig. 5 Post-training increases in hippocampal neurogenesis weakens conditioned place preference for cocaine. a One side of the conditioned place preference (CPP) box was conditioned with saline, and the other side was conditioned with cocaine (7.5 mg/kg) for 3 days training. CPP score was measured 4 weeks after the final training. **b** Exercise suppressed the CPP score (Unpaired *t*-test, $t_{39} = 2.58$, $P = 0.014$). **c** $Nestin^+$ cells were stimulated optogenetically after CPP training to promote re-organization of hippocampal neuronal circuits in Nestin-CreERT2 ChR2 mice. **d** The $ChR2^+$ group showed a decreased CPP score (Mann-Whitney *U*-test, $U = 57$, $P = 0.0037$). **e** Neuronal re-organization was induced by tamoxifen injection in Nestin-CreERT2 $Sema5A^{-/-}$ mice after CPP training. **f** $Sema5A^{-/-}$ group decreased CPP score (Unpaired *t*-test, $t_{16} = 2.58$, $P = 0.020$). Data are represented as mean ± S.E.M. Data points represent individual mice (**b**; Sed, n = 20, Run, n = 21, **d**; $ChR2^-$ mice n = 16, $ChR2^+$ mice n = 17, **f**; $Sema5A^{+/+}$ mice, n = 11, $Sema5A^{-/-}$ mice, n = 7). Statistical significance is indicated by asterisks.

circuits. The same interventions also weakened cocaine place preference memories, suggesting that promoting hippocampal neurogenesis may represent a useful approach for addressing persistent maladaptive memories in hypermnesic conditions such as PTSD and addiction.

In adult rodents, increasing hippocampal neurogenesis following training induces forgetting of hippocampus-dependent, but not hippocampus-independent, memories [14–19]. These effects have been observed in a broad range of appetitively- and aversively-motivated tasks, including contextual fear conditioning [14, 15, 17–19], inhibitory avoidance [18], water maze [14, 16], Barnes maze [14], and odor-context paired associate learning [16]. The current findings extend this pattern to a rodent model for PTSD. This paradigm [26] involves two traumatic events, with animals first trained in an inhibitory avoidance task using a high intensity footshock (event 1). Subsequent presentation of a reminder shock in a different context (event 2) then strengthens the original trauma memory, and leads to the emergence of a constellation of other behaviors that mimic those observed in PTSD.

Several features of this paradigm make it suitable for modeling PTSD in rodents. First, the initial trauma experience is high intensity, and induces changes in corticosterone levels in the circulation [26]. Second, behavioral changes are not restricted to the original memory. Rather, the reminder shock elicits a broad range of behavioral changes, including increased anxiety, increased threat generalization, and impaired extinction. Third, these behavioral changes linger, and are evident up to 1 month following the original trauma. This paradigm is also suitable for examining the impact manipulations of hippocampal neurogenesis since the hippocampus plays a central role in the formation and maintenance of IA memories. For example, training in this paradigm induces changes in plasticity markers in the hippocampus [26], whereas inactivation of the hippocampus prevents acquisition and expression of IA memories [47].

In our experiments we used both specific (i.e., targeting neural progenitor cells) and non-specific (i.e., exercise) approaches to manipulate hippocampal neurogenesis. Interestingly, exercise appeared to have broader impact on PTSD-related phenotypes in our model, modulating extinction, threat generalization, and anxiety-like phenotypes. In contrast, specific interventions that selectively induced hyper-integration of newly-generated granule cells (optogenetic stimulation of newly-generated granule cells or neural progenitor cell-specific deletion of Sema5A) had more selective effects. These interventions modulated extinction and threat generalization behaviors, but were less effective in reducing anxiety. An emerging picture is that the hippocampus is a functionally heterogeneous structure along its longitudinal axis [48], with the dorsal hippocampus more important for memory function and the ventral hippocampus more important for mood/anxiety. One possibility, therefore, is that our manipulations differentially impacted neurogenesis in the dorsal versus ventral hippocampus. Consistent with this, in our optogenetic studies, optical fibers were placed above the dorsal hippocampus raising the possibility that photostimulation preferentially affected the maturation of newly-generated neurons only in the dorsal hippocampus. This possibility can be further evaluated in future work using localized manipulations of hippocampal neurogenesis [6]. Exercise interventions induce changes both within and beyond the hippocampus [43]. Therefore, a second possibility is that exercise-induced changes in extra-hippocampal regions accounts for the more potent effects of exercise on anxiety behaviors in our model.

While exercise may be a relatively non-specific intervention, we note that there is evidence that its effects on memory are mediated via modulation of hippocampal neurogenesis. Exercise-induced forgetting of contextual fear memory [14, 34] and odor-context paired associate memories [16] are blocked by targeted inhibition of hippocampal neurogenesis (either via restricting integration of newborn neurons or by ablation of neural progenitor cells). An advantage of non-specific interventions such as exercise is that is more straightforward to implement in PTSD patient populations and therefore is translationally relevant. Indeed, consistent with our findings using exercise to elevate hippocampal neurogenesis in mice, clinical studies have reported beneficial effects of exercise programs in PTSD patients [37–42]. For example, in a randomized control trial in military veterans with PTSD, an exercise program reduced PTSD and depressive symptoms, and improved sleep [38].

Earlier studies also explored the impact of manipulating hippocampal neurogenesis in PTSD-related paradigms. In one study, post-training exercise or systemic treatment with the proneurogenic drug memantine (a non-competitive inhibitor of N-Methyl-D-Aspartate [NMDA] glutamate receptors) increased hippocampal neurogenesis and led to forgetting of IA and contextual fear memories [18]. In another study, memantine had similarly beneficial effects in a social defeat paradigm, reducing social avoidance and anxiety-like behaviors [36]. While these data are consistent with those in the current study, two limitations are worth noting. First, as an NMDA inhibitor, memantine likely induces a large number of neural and physiological changes other than increasing neurogenesis that might also contribute to forgetting. Second, conventional IA and contextual fear conditioning paradigms are likely insufficiently intense and therefore incompletely recapitulate behavioral changes associated with PTSD (such as deficient extinction, anxiety-like behavior) [49, 50]. The current results address these limitations by (a) restricting manipulations to neural progenitor cells and their progeny and (b) using a more intense behavioral paradigm to model PTSD that produces lingering changes up to 1 month following initial trauma. In doing so, they establish a direct causal link between hippocampal neurogenesis and the resulting alterations PTSD-like behaviors. Moreover, we found a similar pattern of results in the cocaine place preference paradigm, with post-training proneurogenic interventions inducing forgetting. These results extend earlier studies using nonspecific proneurogenic interventions [51, 52] (but see: [53]).

How might increasing hippocampal neurogenesis attenuate trauma and addiction memories in mice? Memory formation involves the strengthening of synaptic connections among neuronal ensembles (or engrams) that are co-active during encoding, and subsequent engram reactivation then leads to successful memory retrieval [54]. Three lines of evidence for this model have emerged from engram tagging studies [54–56]. First, neuronal ensembles that are active at encoding are reactivated at above chance rates during retrieval of the corresponding memory. Second, inhibition of neuronal ensembles that are active at encoding disrupt memory retrieval (in the presence of cues that would normally support successful recall). Third, activation of neuronal ensembles that are active at encoding are sufficient to induce memory retrieval (in the absence of cues that would normally support successful recall). According to this model, forgetting occurs when neural circuit alterations reduce engram accessibility, and hence the probability of engram reactivation [57].

As new neurons integrate into hippocampal circuits, they receive input connections from perforant path and form output connections onto CA3 pyramidal neurons via large mossy fiber terminals. During this period, new input and output synaptic connections may co-exist with or eventually replace established synaptic connections [3–5]. Amidst this remodeling, we hypothesize that engram accessibility is reduced. Experiments using a contextual fear paradigm provide several observations that are consistent with this view [34]. First, post-training interventions that promote hyper-integration of newborn neurons into hippocampal circuits (e.g., optogenetic activation

of nestin$^+$ cells in DG, deletion of Sema5A from neural progenitor cells) induce forgetting (without altering survival of newborn neurons) [34]. Second, post-training interventions that impede integration of newborn neurons into hippocampal circuits (e.g., deletion of cadherin 9 A or Rac1 from neural progenitor cells) prevent exercise-induced forgetting [34]. Third, using engram tagging approaches, post-training exercise reduced reactivation of tagged 'engram' neurons in CA3 and CA1 and produced forgetting of contextual fear memories. Using similar methods, reduced engram reactivation was also associated with forgetting of contextual fear memories during development when levels of hippocampal neurogenesis are elevated [58].

In the current study, we did not use engram tagging approaches to label hippocampal ensembles underlying the trauma memories. However, engram tagging approaches have been used in a related social defeat paradigm [59], in which a mouse is repeatedly attacked (or defeated) by an aggressor mouse. In this study, engram tagging occurred during this initial social defeat phase, and then mice were re-exposed to the aggressor mouse. In mice that exhibited susceptible behavioral phenotypes, hippocampal engram reactivation rates were high. In contrast, in mice that exhibited resilient behavioral phenotypes, hippocampal engram reactivation rates were low. Consistent with our reasoning here, these results suggest that reduced engram reactivation is associated with weaker memory expression.

In developing interventions to treat PTSD, there has been considerable interest in targeting post-encoding processes that alter memory expression, such as extinction, reconsolidation, and extinction-reconsolidation [60, 61]. For example, drugs that enhance extinction [62] or impair reconsolidation [63, 64] may be useful pharmacotherapeutic adjuncts in prolonged exposure therapy. The current experiments indicate that targeting another post-encoding memory process—forgetting—offers promise for treatment of hypermnesic conditions such as PTSD and addiction. One important limitation for forgetting-based approaches is worth noting, however. Extinction, extinction-reconsolidation, and reconsolidation strategies allow 'active' memories (i.e., the reactivated trauma memory) to be targeted and so offer greater specificity. In contrast, forgetting-based approaches do not involve reactivation of the original trauma experience and potentially may additionally impact both positively- and negatively-valenced 'off-target' memories. This was not addressed in the current study.

While we focused on neurogenesis-mediated forgetting, forgetting encompasses a broad collection of mechanisms that all function to reduce engram accessibility [57, 65, 66]. Therefore future preclinical studies may address whether targeting other forgetting mechanisms—including receptor trafficking [67], microglial activation [19], changes in E/I balance [68], and Rac1-dependent intracellular signaling [69]—offer additional approaches for weakening maladaptive memories in hypermnesic conditions such as PTSD and addiction.

DATA AVAILABILITY

The data that were used to support the findings of this study are available from the corresponding author upon request.

REFERENCES

1. Goncalves JT, Schafer ST, Gage FH. Adult neurogenesis in the hippocampus: from stem cells to behavior. Cell. 2016;167:897–914. https://doi.org/10.1016/j.cell.2016.10.021
2. Kempermann G, Gage FH, Aigner L, Song H, Curtis MA, Thuret S, et al. Human adult neurogenesis: evidence and remaining questions. Cell Stem Cell. 2018;23:25–30. https://doi.org/10.1016/j.stem.2018.04.004
3. McAvoy KM, Scobie KM, Berger S, Russo C, Guo N, Decharatanachart P, et al. Modulating neuronal competition dynamics in the dentate gyrus to rejuvenate aging memory circuits. Neuron. 2016;91:1356–73. https://doi.org/10.1016/j.neuron.2016.08.009
4. Toni N, Laplagne DA, Zhao C, Lombardi G, Ribak CE, Gage FH, et al. Neurons born in the adult dentate gyrus form functional synapses with target cells. Nat Neurosci. 2008;11:901–7. https://doi.org/10.1038/nn.2156
5. Toni N, Teng EM, Bushong EA, Aimone JB, Zhao C, Consiglio A, et al. Synapse formation on neurons born in the adult hippocampus. Nat Neurosci. 2007;10:727–34. https://doi.org/10.1038/nn1908
6. Anacker C, Hen R. Adult hippocampal neurogenesis and cognitive flexibility—linking memory and mood. Nat Rev Neurosci. 2017;18:335–46. https://doi.org/10.1038/nrn.2017.45
7. Clelland CD, Choi M, Romberg C, Clemenson GD, Fragniere A, Tyers P, et al. A functional role for adult hippocampal neurogenesis in spatial pattern separation. Science. 2009;325:210–3. https://doi.org/10.1126/science.1173215
8. Sahay A, Scobie KN, Hill AS, O'Carroll CM, Kheirbek MA, Burghardt NS, et al. Increasing adult hippocampal neurogenesis is sufficient to improve pattern separation. Nature. 2011;472:466–70. https://doi.org/10.1038/nature09817
9. Niibori Y, Yu TS, Epp JR, Akers KG, Josselyn SA, Frankland PW. Suppression of adult neurogenesis impairs population coding of similar contexts in hippocampal CA3 region. Nat Commun. 2012;3:1253 https://doi.org/10.1038/ncomms2261
10. Deisseroth K, Singla H, Toda H, Monje M, Palmer TD, Malenka RC. Excitation-neurogenesis coupling in adult neural stem/progenitor cells. Neuron. 2004;42:535–52. https://doi.org/10.1016/s0896-6273(04)00266-1
11. Tran LM, Josselyn SA, Richards BA, Frankland PW. Forgetting at biologically realistic levels of neurogenesis in a large-scale hippocampal model. Behav Brain Res. 2019;376:112180 https://doi.org/10.1016/j.bbr.2019.112180
12. Weisz VI, Argibay PF. Neurogenesis interferes with the retrieval of remote memories: forgetting in neurocomputational terms. Cognition. 2012;125:13–25. https://doi.org/10.1016/j.cognition.2012.07.002
13. Frankland PW, Kohler S, Josselyn SA. Hippocampal neurogenesis and forgetting. Trends Neurosci. 2013;36:497–503. https://doi.org/10.1016/j.tins.2013.05.002
14. Akers KG, Martinez-Canabal A, Restivo L, Yiu AP, De Cristofaro A, Hsiang HL, et al. Hippocampal neurogenesis regulates forgetting during adulthood and infancy. Science. 2014;344:598–602. https://doi.org/10.1126/science.1248903
15. Cuartero MI, de la Parra J, Perez-Ruiz A, Bravo-Ferrer I, Duran-Laforet V, Garcia-Culebras A, et al. Abolition of aberrant neurogenesis ameliorates cognitive impairment after stroke in mice. J Clin Investig. 2019;129:1536–50. https://doi.org/10.1172/JCI120412
16. Epp JR, Silva Mera R, Kohler S, Josselyn SA, Frankland PW. Neurogenesis-mediated forgetting minimizes proactive interference. Nat Commun. 2016;7:10838 https://doi.org/10.1038/ncomms10838
17. Gao A, Xia F, Guskjolen AJ, Ramsaran AI, Santoro A, Josselyn SA, et al. Elevation of hippocampal neurogenesis induces a temporally graded pattern of forgetting of contextual fear memories. J Neurosci. 2018;38:3190–8. https://doi.org/10.1523/JNEUROSCI.3126-17.2018
18. Ishikawa, R, Fukushima, H, Frankland, PW & Kida, S Hippocampal neurogenesis enhancers promote forgetting of remote fear memory after hippocampal reactivation by retrieval. Elife 5 https://doi.org/10.7554/eLife.17464 (2016).
19. Wang C, Yue H, Hu Z, Shen Y, Ma J, Li J, et al. Microglia mediate forgetting via complement-dependent synaptic elimination. Science. 2020;367:688–94. https://doi.org/10.1126/science.aaz2288
20. Epp JR, Botly LCP, Josselyn SA, Frankland PW. Voluntary exercise increases neurogenesis and mediates forgetting of complex paired associates memories. Neuroscience. 2021;475:1–9. https://doi.org/10.1016/j.neuroscience.2021.08.022
21. Scott GA, Terstege DJ, Roebuck AJ, Gorzo KA, Vu AP, Howland JG, et al. Adult neurogenesis mediates forgetting of multiple types of memory in the rat. Mol Brain. 2021;14:97 https://doi.org/10.1186/s13041-021-00808-4
22. Evans A, Terstege DJ, Scott GA, Tsutsui M, Epp JR. Neurogenesis mediated plasticity is associated with reduced neuronal activity in CA1 during context fear memory retrieval. Sci Rep. 2022;12:7016 https://doi.org/10.1038/s41598-022-10947-w
23. Dunsmoor JE, Paz R. Fear generalization and anxiety: behavioral and neural mechanisms. Biol. Psychiatry. 2015;78:336–43.
24. Orr SP, Metzger LJ, Lasko NB, Macklin ML, Peri T, Pitman RK. De novo conditioning in trauma-exposed individuals with and without posttraumatic stress disorder. J Abnorm. Psychol. 2000;109:290.
25. Rothbaum BO, Kozak MJ, Foa EB, Whitaker DJ. Posttraumatic stress disorder in rape victims: autonomic habituation to auditory stimuli. J Trauma Stress. 2001;14:283–93.
26. Finsterwald C, Steinmetz AB, Travaglia A, Alberini CM. From memory impairment to posttraumatic stress disorder-like phenotypes: the critical role of an unpredictable second traumatic experience. J Neurosci. 2015;35:15903–15. https://doi.org/10.1523/JNEUROSCI.0771-15.2015

27. Imayoshi I, Sakamoto M, Ohtsuka T, Takao K, Miyakawa T, Yamaguchi M, et al. Roles of continuous neurogenesis in the structural and functional integrity of the adult forebrain. Nature neuroscience. 2008;11:1153–61.
28. Duan Y, Wang S-H, Song J, Mironova Y, Ming G-l, Kolodkin AL, et al. Semaphorin 5A inhibits synaptogenesis in early postnatal-and adult-born hippocampal dentate granule cells. Elife. 2014;3:e04390.
29. Lewis PF, Emerman M. Passage through mitosis is required for oncoretroviruses but not for the human immunodeficiency virus. J Virol. 1994;68:510–6.
30. Tashiro A, Zhao C, Gage FH. Retrovirus-mediated single-cell gene knockout technique in adult newborn neurons in vivo. Nat. Protoc. 2006;1:3049–55.
31. Zhao C, Teng EM, Summers RG, Ming G-L, Gage FH. Distinct morphological stages of dentate granule neuron maturation in the adult mouse hippocampus. J Neurosci. 2006;26:3–11.
32. Restivo L, Niibori Y, Mercaldo V, Josselyn SA, Frankland PW. Development of adult-generated cell connectivity with excitatory and inhibitory cell populations in the hippocampus. J Neurosci. 2015;35:10600–12.
33. Stone SS, Teixeira CM, Zaslavsky K, Wheeler AL, Martinez-Canabal A, Wang AH, et al. Functional convergence of developmentally and adult-generated granule cells in dentate gyrus circuits supporting hippocampus-dependent memory. Hippocampus. 2011;21:1348–62.
34. Guskjolen A, Dhaliwal J, de la Parra J, Epp JR, Ko S, Chahley E, et al. Neurogenesis-mediated circuit remodeling reduces engram reinstatement and promotes forgetting. *bioRxiv*, 2023.2010. 2010.561722 (2023).
35. Hsiang H-LL, Epp JR, van den Oever MC, Yan C, Rashid AJ, Insel N, et al. Manipulating a "cocaine engram" in mice. J Neurosci. 2014;34:14115–27.
36. Ishikawa R, Uchida C, Kitaoka S, Furuyashiki T, Kida S. Improvement of PTSD-like behavior by the forgetting effect of hippocampal neurogenesis enhancer memantine in a social defeat stress paradigm. Mol Brain. 2019;12:68 https://doi.org/10.1186/s13041-019-0488-6
37. Diaz AB, Motta R. The effects of an aerobic exercise program on posttraumatic stress disorder symptom severity in adolescents. Int J Emerg Ment Health. 2008;10:49–59.
38. Hall KS, Morey MC, Bosworth HB, Beckham JC, Pebole MM, Sloane R, et al. Pilot randomized controlled trial of exercise training for older veterans with PTSD. J Behav Med. 2020;43:648–59. https://doi.org/10.1007/s10865-019-00073-w
39. Hegberg NJ, Hayes JP, Hayes SM. Exercise intervention in PTSD: a narrative review and rationale for implementation. Front Psychiatry. 2019;10:133 https://doi.org/10.3389/fpsyt.2019.00133
40. Manger TA, Motta RW. The impact of an exercise program on posttraumatic stress disorder, anxiety, and depression. Int J Emerg Ment Health. 2005;7:49–57.
41. Powers MB, Medina JL, Burns S, Kauffman BY, Monfils M, Asmundson GJ, et al. Exercise augmentation of exposure therapy for PTSD: rationale and pilot efficacy data. Cogn Behav Ther. 2015;44:314–27. https://doi.org/10.1080/16506073.2015.1012740
42. Shivakumar G, Anderson EH, Suris AM, North CS. Exercise for PTSD in women veterans: a proof-of-concept study. Mil Med. 2017;182:e1809–e1814. https://doi.org/10.7205/MILMED-D-16-00440
43. Hillman CH, Erickson KI, Kramer AF. Be smart, exercise your heart: exercise effects on brain and cognition. Nat Rev Neurosci. 2008;9:58–65. https://doi.org/10.1038/nrn2298
44. Crombag HS, Bossert JM, Koya E, Shaham Y. Context-induced relapse to drug seeking: a review. Philos Trans R Soc B Biol Sci. 2008;363:3233–43.
45. Tzschentke TM. Measuring reward with the conditioned place preference (CPP) paradigm: update of the last decade. Addict Biol. 2007;12:227–462. https://doi.org/10.1111/j.1369-1600.2007.00070.x
46. Napier TC, Herrold AA, de Wit H. Using conditioned place preference to identify relapse prevention medications. Neurosci Biobehav Rev. 2013;37:2081–6. https://doi.org/10.1016/j.neubiorev.2013.05.002
47. Lorenzini CA, Baldi E, Bucherelli C, Sacchetti B, Tassoni G. Role of dorsal hippocampus in acquisition, consolidation and retrieval of rat's passive avoidance response: a tetrodotoxin functional inactivation study. Brain Res. 1996;730:32–39.
48. Kheirbek MA, Drew LJ, Burghardt NS, Constantini DO, Tannenholz L, Ahmari SE, et al. Differential control of learning and anxiety along the dorsoventral axis of the dentate gyrus. Neuron. 2013;77:955–68.
49. Richter-Levin G, Stork O, Schmidt MV. Animal models of PTSD: a challenge to be met. Mol Psychiatry. 2019;24:1135–56. https://doi.org/10.1038/s41380-018-0272-5
50. Desmedt A, Marighetto A, Piazza PV. Abnormal fear memory as a model for posttraumatic stress disorder. Biol Psychiatry. 2015;78:290–7. https://doi.org/10.1016/j.biopsych.2015.06.017
51. Ladron de Guevara-Miranda D, Moreno-Fernandez RD, Gil-Rodriguez S, Rosell-Valle C, Estivill-Torrus G, Serrano A, et al. Lysophosphatidic acid-induced increase in adult hippocampal neurogenesis facilitates the forgetting of cocaine-contextual memory. Addict Biol. 2019;24:458–70. https://doi.org/10.1111/adb.12612
52. Mustroph ML, Stobaugh DJ, Miller DS, DeYoung EK, Rhodes JS. Wheel running can accelerate or delay extinction of conditioned place preference for cocaine in male C57BL/6J mice, depending on timing of wheel access. Eur J Neurosci. 2011;34:1161–9. https://doi.org/10.1111/j.1460-9568.2011.07828.x
53. Mustroph ML, Merritt JR, Holloway AL, Pinardo H, Miller DS, Kilby CN, et al. Increased adult hippocampal neurogenesis is not necessary for wheel running to abolish conditioned place preference for cocaine in mice. Eur J Neurosci. 2015;41:216–26. https://doi.org/10.1111/ejn.12782
54. Frankland PW, Josselyn SA, Kohler S. The neurobiological foundation of memory retrieval. Nat Neurosci. 2019;22:1576–85. https://doi.org/10.1038/s41593-019-0493-1
55. Josselyn SA, Kohler S, Frankland PW. Finding the engram. Nat Rev Neurosci. 2015;16:521–34. https://doi.org/10.1038/nrn4000
56. Josselyn SA, Tonegawa S. Memory engrams: recalling the past and imagining the future. *Science* 2020; 367 https://doi.org/10.1126/science.aaw4325
57. Ryan TJ, Frankland PW. Forgetting as a form of adaptive engram cell plasticity. Nat Rev Neurosci. 2022;23:173–86.
58. Guskjolen A, Kenney JW, de la Parra J, Yeung BA, Josselyn SA, Frankland PW. Recovery of "Lost" Infant Memories in Mice. Curr Biol. 2018;28:2283–2290.e2283. https://doi.org/10.1016/j.cub.2018.05.059
59. Zhang TR, Larosa A, Dr Raddo ME, Wong V, Wong AS, Wong TP. Negative memory engrams in the hippocampus enhance the susceptibility to chronic social defeat stress. J Neurosci. 2019;39:7576–90. https://doi.org/10.1523/JNEUROSCI.1958-18.2019
60. Kida S. Reconsolidation/destabilization, extinction and forgetting of fear memory as therapeutic targets for PTSD. Psychopharmacology. 2019;236:49–57. https://doi.org/10.1007/s00213-018-5086-2
61. Phelps EA, Hofmann SG. Memory editing from science fiction to clinical practice. Nature. 2019;572:43–50. https://doi.org/10.1038/s41586-019-1433-7
62. Michopoulos V, Norrholm SD, Stevens JS, Glover EM, Rothbaum BO, Gillepsie CF, et al. Dexamethasone facilitates fear extinction and safety discrimination in PTSD: a placebo-controlled, double-blind study. Psychoneuroendocrinology. 2017;83:65–71. https://doi.org/10.1016/j.psyneuen.2017.05.023
63. Brunet A, Orr SP, Tremblay J, Robertson K, Nader K, Pitman RK. Effect of post-retrieval propranolol on psychophysiologic responding during subsequent script-driven traumatic imagery in post-traumatic stress disorder. J Psychiatr Res. 2008;42:503–6. https://doi.org/10.1016/j.jpsychires.2007.05.006
64. Soeter M, Kindt M. An abrupt transformation of phobic behavior after a post-retrieval amnesic agent. Biol Psychiatry. 2015;78:880–6. https://doi.org/10.1016/j.biopsych.2015.04.006
65. Davis RL, Zhong Y. The biology of forgetting-A perspective. Neuron. 2017;95:490–503. https://doi.org/10.1016/j.neuron.2017.05.039
66. Richards BA, Frankland PW. The persistence and transience of memory. Neuron. 2017;94:1071–84. https://doi.org/10.1016/j.neuron.2017.04.037
67. Hardt O, Nader K, Wang YT. GluA2-dependent AMPA receptor endocytosis and the decay of early and late long-term potentiation: possible mechanisms for forgetting of short- and long-term memories. Philos Trans R Soc Lond B Biol Sci. 2014;369:20130141 https://doi.org/10.1098/rstb.2013.0141
68. Barron HC, Vogels TP, Behrens TE, Ramaswami M. Inhibitory engrams in perception and memory. Proc Natl Acad Sci USA. 2017;114:6666–74. https://doi.org/10.1073/pnas.1701812114
69. Shuai Y, Zhong Y. Forgetting and small G protein Rac. Protein Cell. 2010;1:503–6. https://doi.org/10.1007/s13238-010-0077-z

ACKNOWLEDGEMENTS

This work was supported by a CIHR project grant (PJT-180530) to PWF, and Brain Canada platform, and NIMH grants (RO1MH119421) to SAJ and PWF Additionally we acknowledge generous support from the Brenneman family and the SickKids Foundation. RF was supported by JSPS KAKENHI Grant Number 14J05605, The Kyoto University Foundation, Astellas Foundation for Research on Metabolic Disorders, and SENSHIN Medical Research Foundation. AIR was supported by an NSERC CGS-D award and an NIH 1 F31 MH120920-01 award. We thank Ms. Daisy Lin, Ms. Toni DeCristofaro, and Ms. Mika Yamamoto for technical assistance.

AUTHOR CONTRIBUTIONS

RF: Conceptualization, Data Collection, Statistical Analysis, Writing (Original Draft), Writing (Editing). AIR: Data Collection, Statistical Analysis, Writing (Editing). AG: Data Collection, Writing (Editing). JDLP: Data Collection, Writing (Editing). YZ: Data Collection. AJM: Data Collection, Writing (Editing). SAJ: Supervision, Funding, Writing (Editing). PWF: Conceptualization, Supervision, Funding, Writing (Original Draft), Writing (Editing).

COMPETING INTERESTS

The authors declare no competing interests.

ADDITIONAL INFORMATION

Supplementary information The online version contains supplementary material available at https://doi.org/10.1038/s41380-024-02585-7.

Correspondence and requests for materials should be addressed to Paul W. Frankland.